

New phenoxy methyl substituted mesoionic triazolium salts: Synthesis and structural characterisation

George Dhimba, Nasir S. Lawal, Muhammad D. Bala*

School of Chemistry and Physics, University of KwaZulu-Natal, Private Bag X54001, Durban 4000, South Africa

ARTICLE INFO

Article history:

Received 23 August 2018

Received in revised form

26 October 2018

Accepted 31 October 2018

Available online 1 November 2018

Keywords:

Triazolium salt

Click chemistry

X-ray diffraction

Metal-free catalyst

ABSTRACT

A new set of mesoionic 1,2,3-triazolium salts functionalised by *para* substituted phenoxy methyl side groups were prepared using the 'click' Cu catalyzed [3 + 2] cycloaddition of organic azides and terminal alkynes. Four previously unreported neutral triazoles (**1–4**) were first isolated en route to formation of the salts (**5–8**). All the compounds were fully characterised (¹H, ¹³C NMR; IR; HR-MS; EA) and representative neutral triazoles and salts were structurally characterised by single crystal X-ray diffraction (SCXRD). Full examination of structural characteristics of the neutral compounds and the salts were presented by detailed analysis of multinuclear NMR data and SCXRD. As metal-free catalysts for the transfer hydrogenation of ketones to alcohols in isopropanol as solvent and hydrogen source, salts **5–8** showed moderate activities for the transformation of acetophenone to 1-phenyl alcohol.

© 2018 Elsevier B.V. All rights reserved.

1. Introduction

Since the versatile “green” concept of “click” reaction was first coined and defined by Kolb, Finn and Sharpless in 2001, the chemistry of mesoionic 1,2,3-triazolium salts has evolved over the years [1]. This is due to the possibility of functionalizing the triazole ring with a wide range of wingtip (N1 and C4) substituents, thereby providing stability and extending the scope of triazolium *N*-heterocyclic chemistry [2]. This opportunity makes it possible for fine-tuning the triazole ring to suit a variety of chemical applications including use as ionic liquids, as organocatalysts and as ligands for organometallic synthesis [3]. Compared with imidazolium salts, triazolium salts tend to be more stable, because the former are inherently limited by their acidic C(2)–H proton which is very susceptible to deprotonation in the presence of strong bases, thereby generating reactive carbenes, the well-publicized *N*-heterocyclic carbenes (NHC) [4]. In addition, triazolium ligands are gradually been accepted as alternative ligands to the imidazolium variants in organometallic chemistry and homogeneous catalysis [5,6]. This is due to the ease of their synthesis via the highly efficient route of ‘click’ [3 + 2] cycloaddition reactions which has also expanded their scope as ionic liquids, anti-microbial agents and materials [7].

Also, in an effort to develop much cheaper, sustainable and environmentally benign catalyst systems, we recently reported a set of imidazolium based organocatalysts for the transfer hydrogenation (TH) of ketones [8]. Herein, we report new phenoxy methyl substituted triazolium salts synthesized via Cu(I) catalyzed azide/alkyne cycloaddition, for use as potential sources of NHC ligands and also demonstrated their potential as organocatalyst in TH of acetophenone.

2. Experimental

All chemicals and reagents were of reagent grade and were used as purchased. All NMR spectra were recorded in deuterated solvents using a Bruker Ultra-Shield™ spectrometer AVANCEIII operating at a frequency of 400 MHz and ambient temperature. Chemical shifts were recorded as δ values in reference to SiMe₃ at 0.00 parts per million (ppm) at 25 °C. ¹H NMR were reported as: chemical shift (δ , ppm) and referenced to the solvent peak CDCl₃ (7.26 ppm); multiplicity and number of protons are presented in parentheses. The proton decoupled ¹³C NMR was conducted to obtain the carbon skeleton of the triazoles and was presented as: chemical shift (δ , ppm) and referenced to the solvent peak CDCl₃ (77.16 ppm) with the specific carbon indicated in parentheses. The IR spectra were recorded on a Perkin Elmer Attenuated Total Reflectance (ATR) spectrophotometer in the 4000–400 cm⁻¹ region. Melting point measurements were performed using a Stuart Scientific melting point apparatus. The mass-to-charge ratio (*m/z*) of

* Corresponding author.

E-mail address: bala@ukzn.ac.za (M.D. Bala).

the compounds was determined using a Bruker Micro TOF-Q11 mass spectrometry with electron spray ionisation (ESI) and a sample concentration of approximately 1 ppm.

2.1. General procedure for the synthesis of 1,2,3-triazole based compounds 1–8

Scheme 1 illustrates the typical route for the synthesis of the 1,2,3-triazoles **1–4** and their corresponding salts **5–8**. Thus, the general procedure for the synthesis of **1–4** is described: In a 100 ml round bottomed flask containing acetone (30 ml) was transferred *p*-nitro phenol (1.500 g, 10.8 mmol), propargyl bromide (1.28 g, 10.8 mmol) and K_2CO_3 (2.99 g, 21.6 mmol). The mixture was stirred under reflux for 18 h, then cooled to room temperature and filtered over a pad of Celite. The crude filtrate was concentrated under reduced pressure and added to 1 mol equivalent of *in situ* generated organic azide. Then aqueous solutions of CuBr (5%), sodium ascorbate (10%) and 5 ml H_2O were added. The mixture was stirred for a further 18 h at room temperature. The resulting suspension was partitioned between aqueous $NH_4OH/EDTA$ (100 ml) and CH_2Cl_2 (100 ml). The organic layer was separated and washed with H_2O (100 ml), then dried over $MgSO_4$. All volatiles were removed under reduced pressure to yield solids that were characterised and confirmed as products **1–4**.

In a typical *N*-alkylation procedure (**Scheme 1**), 0.500 g of a triazole (**1–4**) was added into a round bottomed flask, followed by 10 ml of acetonitrile and 1.2 equiv. of methyl iodide, the reaction was stirred under reflux at 80 °C for 18 h. Excess methyl iodide and solvent were removed by vacuum distillation. The crude salt was then precipitated with dry ethyl acetate followed by filtration to correspondingly afford triazolium salts (**5–8**) in moderate to high yields.

2.1.1. 1-Butyl-4-((4-nitrophenoxy)methyl)-1H-1, 2, 3-triazole (1)

Yellow crystals, 62.6% yield, mp 64–66 °C. 1H NMR (400 MHz, $CDCl_3$, ppm): δ 8.22–8.20 (q, 2H, Ar) 7.63 (s, 1H, triazole, C=CH), 7.10–7.07 (m, 2H, Ar) 5.31 (s, 2H, CH_2), 4.40–4.36 (t, 2H, CH_2) 1.95–1.87 (q, 2H, CH_2) 1.42–1.32 (m, 2H, CH_2) 0.98–0.94 (t, 3H, CH_3) ^{13}C NMR (100 MHz, $CDCl_3$, ppm): δ 163.1, 142.7, 141.9, 125.9, 122.7, 114.8, 62.5, 50.3, 32.2, 19.7, 13.4; IR (ATR, cm^{-1}): 3150, 3086, 2956, 2438, 2119, 1979, 1745, 1660, 1552, 1593, 1512, 1496, 1465; HRMS calcd for $C_{13}H_{16}N_4NaO_3$ 299.1120. Found 299.1114. Elem. Anal. Found (calcd) for $C_{13}H_{16}N_4O_3$: C, 56.80 (56.51); N, 21.51 (21.28); H, 5.04 (5.84).

2.1.2. 4-((4-Bromophenoxy)methyl)-1-butyl-1H-1, 2, 3-triazole (2)

White solid, 56% yield, mp 66–67 °C. 1H NMR (400 MHz, $CDCl_3$, ppm): δ 7.57 (s, 1H, triazole, C=CH) 7.40–7.36 (m, 2H, Ar) 6.90–6.86 (m, 2H, Ar) 5.18 (s, 2H, CH_2) 4.38–4.34 (t, 2H, CH_2) 1.93–1.86 (m, 2H, CH_2) 1.41–1.32 (m, 2H, CH_2) 0.98–0.94 (t, 3H,

CH_3) ^{13}C NMR (100 MHz, $CDCl_3$, ppm): δ 157.3, 143.7, 132.3, 122.4, 116.6, 113.4, 62.3, 50.2, 32.2, 19.7, 13.4; IR (ATR, cm^{-1}): 3145, 3107, 3062, 2957, 2874, 2431, 1916, 1890, 1579, 1592, 1491, 1289, 1251. HRMS calcd for $C_{13}H_{16}BrN_3NaO$ 333.0380. Found 332.0380. Elem. Anal. Found (calcd) for $C_{13}H_{16}N_3BrO$: C, 50.47 (50.34); N, 14.23 (13.15); H, 4.80 (5.20).

2.1.3. Ethyl-2-(4-((4-nitrophenoxy)methyl)-1H-1,2,3-triazol-1-yl) acetate (3)

White crystalline solid, 47% yield, mp 110–112 °C. 1H NMR (400 MHz, $CDCl_3$, ppm): δ 8.22–8.20 (q, 2H, Ar) 7.81 (s, 1H, triazole, C=CH) 7.10–7.07 (q, 2H, Ar), 5.34 (s, 2H, CH_2), 5.19 (s, 2H, CH_2), 4.31–4.26 (q, 2H, CH_2), 1.33–1.29 (t, 3H, CH_3) ^{13}C NMR (100 MHz, $CDCl_3$, ppm): δ 166.0, 163.0, 162.5, 143.2, 141.9, 125.8, 124.4, 115.0, 62.6, 50.9, 14.0, IR (ATR, cm^{-1}): 3462, 3263, 2996, 2907, 2451, 1935, 1738, 1607, 1592, 1521, 1343, 1243; HRMS calcd for $C_{13}H_{14}N_4$ 329.0862. Found 329.0869. Elem. Anal. Found (calcd) for $C_{13}H_{14}N_4$: C, 52.98 (52.58); N, 18.34 (18.29); H, 4.61 (4.28).

2.1.4. Ethyl-2-(4-((4-bromophenoxy)methyl)-1H-1,2,3-triazol-1-yl) acetate (4)

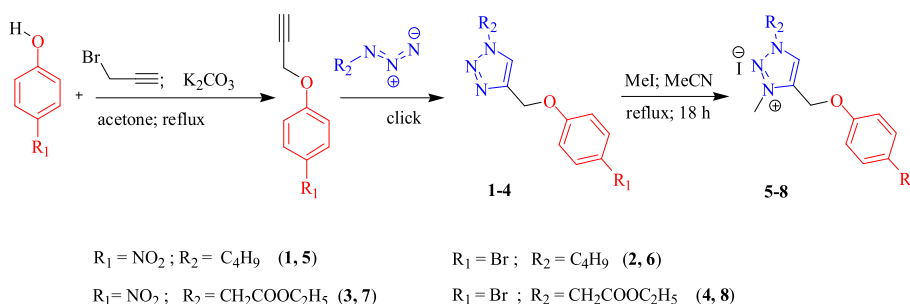
White solid, 38% yield, mp 147–148 °C. 1H NMR (400 MHz, $CDCl_3$, ppm): δ 7.75 (s, 1H, triazole, C=CH), 7.36–7.36 (q, 2H, Ar) 6.90–6.87 (t, 2H, Ar), 5.21 (s, 2H, CH_2), 5.16 (s, 2H, CH_2), 4.30–4.25 (q, 2H, CH_2) 1.32–1.28 (t, 3H, CH_3) ^{13}C NMR (100 MHz, $CDCl_3$, ppm): 166.1, 157.2, 144.3, 132.3, 124.1, 116.6, 113.5, 62.5, 62.1, 50.9, 14.0 IR (ATR, cm^{-1}): 3152, 3098, 2939, 2959, 1892, 1745, 1490, 1240; HRMS calcd for $C_{13}H_{14}BrNaO_3$ 362.0116. Found 362.0110. Elem. Anal. Found (calcd) for $C_{13}H_{14}N_3BrO_3$: C, 47.20 (47.90); N, 12.96 (12.35); H, 3.99 (4.15).

2.1.5. 1-Butyl-3-methyl-4-((4-nitrophenoxy)methyl)-1H-1, 2, 3-triazol-3-ium iodide (5)

Pale yellow solid, 86% yield, mp 129–130 °C. 1H NMR (400 MHz, $CDCl_3$, ppm): δ 9.57 (s, 1H, triazole, C=CH), 8.18–8.16 (d, 2H, Ar) 7.27–7.24 (d, 2H, Ar) 5.87 (s, 2H, CH_2), 4.72–4.51 (t, 2H, CH_2), 4.51 (s, 3H, NCH_3), 2.10–2.02 (m, 2H, CH_2), 1.50–1.40 (m, 2H, CH_2) 1.00–0.97 (t, 3H, CH_3); ^{13}C NMR (100 MHz, $CDCl_3$, ppm): δ 161.4, 142.6, 139.0, 131.4, 126.1, 115.4, 59.9, 54.4, 40.1, 31.2, 19.4, 13.3; IR (ATR, cm^{-1}) 3085, 2998, 2889, 1760, 1747, 1605, 1589, 1509, 1490, 1339, 1235, 1110, 1012, 997, 850; LRMS calcd for $[C_{14}H_{19}N_4O_3]^+$ 291.1457. Found 291.1405. Elem. Anal. Found (calcd) for $C_{14}H_{19}IN_4O_3$: C, 39.91 (40.21); H, 13.22 (13.40); N, 4.53 (4.8).

2.1.6. 4-((4-Bromophenoxy)methyl)-1-butyl-3-methyl-1H-1, 2, 3-triazol-3-ium iodide (6)

White solid, 96% yield, mp 179–181 °C. 1H NMR (400 MHz, $CDCl_3$, ppm): δ 9.54 (s, 1H, triazole, C=CH), 7.43–7.40 (d, 2H, Ar) 7.00–6.98 (d, 2H, Ar) 5.63 (s, 2H, CH_2), 4.69–4.65 (t, 2H, CH_2), 4.44 (s, 3H, NCH_3), 2.07–1.99 (m, 2H, CH_2), 1.46–1.38 (m, 2H, CH_2)



Scheme 1. Click chemistry route to the synthesis of neutral 1,2,3-triazoles (**1–4**) and corresponding salts (**5–8**).

1.00–0.96 (t, 3H, CH₃); ¹³C NMR (100 MHz, CDCl₃, ppm): δ 155.8, 139.5, 132.8, 131.2, 116.8, 116.0, 59.4, 54.3, 39.8, 31.2, 19.4, 13.3; IR (ATR, cm⁻¹) 3084, 2987, 2889, 2185, 1759, 1582, 1487, 1367, 1231, 1158, 1021, 813; LRMS calcd for [C₁₄H₁₉BrN₃O]⁺ 324.0711 Found 324.0726. Elem. Anal. Found (calcd) for C₁₄H₁₉BrN₃O: C, 36.72 (37.19); H, 9.17 (9.29); N, 4.18 (4.24).

2.1.7. 1-(3-Ethoxy-2-oxopropyl)-3-methyl-4-((4-nitrophenoxy)methyl)-1H-1, 2, 3-triazol-3-ium iodide (7)

Pale yellow solid, 53% yield, mp 127–128 °C. ¹H NMR (400 MHz, CDCl₃, ppm): δ 9.58 (s, 1H, triazole C=CH), 8.24–8.22 (d, 2H, Ar) 7.22–7.20 (d, 2H, Ar) 5.80 (s, 2H, CH₂), 5.763 (s, 2H, CH₂) 4.50 (s, 3H, NCH₃), 4.35–4.29 (q, 2H, CH₂), 1.36–1.33 (t, 3H, CH₃); ¹³C NMR (100 MHz, CDCl₃, ppm): δ 164.2, 161.3, 142.8, 138.8, 133.0, 126.2, 115.2, 63.7, 59.7, 54.5, 40.1, 14; IR (ATR, cm⁻¹) 3453, 3041, 2975, 1919, 1749, 1911, 1590, 1511, 1339, 1224, 1109, 1011, 850; LRMS calcd for [C₁₄H₁₇N₄O₅]⁺ 321.1199 Found 321.1208. Elem. Anal. Found (calcd) for C₁₄H₁₇N₄O₅: C, 37.93 (37.52); N, 11.82 (12.50); H, 3.53 (3.82).

2.1.8. 4-((4-Bromophenoxy)methyl)-1-(2-ethoxy-2-oxoethyl)-3-methyl-1H-1, 2, 3-triazol-3-ium iodide (8)

White solid, 51% yield, mp 124–126 °C. ¹H NMR (400 MHz, CDCl₃, ppm): δ 9.55 (s, 1H, triazole C=CH), 7.44–7.42 (d, 2H, Ar) 6.96–6.94 (d, 2H, Ar) 5.77 (s, 2H, CH₂), 5.57 (s, 2H, CH₂) 4.45 (s, 3H, NCH₃), 4.34–4.28 (q, 2H, CH₂), 1.36–1.32 (t, 3H, CH₃); ¹³C NMR (100 MHz, CDCl₃, ppm): δ 164.7, 155.8, 139.3, 132.8, 132.7, 116.7, 63.6, 59.3, 54.5, 40.0, 14; IR (ATR, cm⁻¹) 3443, 3100, 2985, 2914, 2869, 1881, 1757, 1581, 1489, 1230, 1157, 1006, 815; LRMS calcd for [C₁₄H₁₇BrN₃O₃]⁺ 354.0453 Found 354.0399. Elem. Anal. Found (calcd) for C₁₄H₁₇BrN₃O₃: C, 34.34 (34.88); H, 8.59 (8.72); N, 3.44 (3.55).

2.2. X-ray structure determination

Single crystals were selected and glued onto the tip of a glass fiber, mounted in a stream of cold nitrogen at 173 K and centered in the X-ray beam using a video camera. Intensity data were collected on a Bruker APEX II CCD area detector diffractometer with graphite monochromated Mo K α radiation (50 kV, 30 mA) using the APEX 2 data collection software. The collection method involved ω -scans of width 0.5° and 512 × 512 bit data frames. Data reduction was carried out using the program SAINT + while face indexed and multi-scan absorption corrections were made using SADABS. The structures were solved by direct methods using SHELXS [9]. Non-hydrogen atoms were first refined isotropically followed by anisotropic refinement by full matrix least-squares calculations based on F^2 using SHELXS. Hydrogen atoms were first located in the difference map then positioned geometrically and allowed to ride on their respective parent atoms. Diagrams were generated using SHELXTL, PLATON [10] and ORTEP-3 [11]. Crystallographic data for the structures in this article have been deposited with the Cambridge Crystallographic Data Centre, CCDC 1541766–1541769 for **1**, **3**, **6**, and **8** respectively. These data can be obtained free of charge at <http://www.ccdc.cam.ac.uk/conts/retrieving.html> (or from the Cambridge Crystallographic Data Centre, 12 Union Road Cambridge CB2 1EZ, UK; Fax: +44–1223/336–033; E-mail: deposit@ccdc.cam.ac.uk).

3. Results and discussion

The strategy adopted for the synthesis of the disubstituted triazoles allowed for changes in the types of substituents at positions 1 and 4 (so-called wingtip) of the heterocyclic ring aimed at probing electronic and steric influences. We adopted a procedure reported by Luo et al., [12] to synthesize four new triazoles **1–4**. The

compounds were obtained via standard copper(I)-catalyzed alkyne-azide cycloaddition (CuAAC) “click” reactions of *in situ* generated organic azides with terminal alkynes obtained from the reaction of propargyl bromide and *para* substituted phenols (Scheme 1). Due to safety concerns associated with the handling and isolation of azides bearing short-chain low molecular weight alkyl groups, isolation of the organic azides was avoided. They are well-known to be highly energetic and potentially explosive at high concentrations [13] hence the cycloaddition reactions were conducted *in situ* with crude concentrates of previously generated alkynes. The triazoles were isolated in moderate yields and were *N*-alkylated in a simple and straightforward protocol depicted in Scheme 1. The Quaternisation step usually conducted in polar aprotic solvents such as acetonitrile was achieved under mild conditions without the need for an inert atmosphere or any special precautions affording moderate to high yields of salts **5–8** [14,15].

All new compounds were fully characterised by spectroscopic and analytical techniques. Well-resolved NMR spectra were obtained for the triazoles and corresponding *N*-quaternised salts. For instance, the proton NMR spectrum of **1** showed the typical triazole fingerprint proton pattern at 7.63 ppm (Fig. 1), while the proton decoupled ¹³C NMR spectrum showed the typical triazole ring C(5) resonance signal at 123 ppm (see the ESI), which is consistent with reported literature assignments for triazoles [16].

Quaternisation of **1** to the corresponding triazolium salt (**5**) was confirmed by the appearance of a singlet signal at 4.51 ppm which integrated to 3 protons for methyl alkylation. Downfield shift of the C(5)–H proton to 9.57 ppm also confirmed successful *N*-alkylation (Fig. 2) [17,18]. Downfield shifts in carbon resonance positions was also observed in the ¹³C NMR spectra of all the salts when compared to corresponding neutral triazoles with an average of 5 ppm shift in resonance positions (see ESI). For all the salts, the selective alkylation and quaternisation of the more nucleophilic N(3) was observed and is confirmed by 2D ¹H–¹H NOESY NMR analysis [19,20].

Generally, NOE cross peaks are caused by cross relaxation between adjacent protons that are spatially in close proximity (approximately less than 5 Å apart) [21]. For example the NOESY spectrum of **7** (Fig. 3) showed NOE correlations between the methyl protons bonded to N(3) and methylene protons bonded to the phenoxy ring, suggesting that they are in close proximity, a result that is in harmony with findings on similar compounds reported in the literature [17].

Calculated *m/z* values for all the compounds correlated well with observed values, while the fragmentation patterns showed peaks at [M]⁺ (100% abundance) and [M+1]⁺ (1.1% abundance) which are attributed to the ¹²C and ¹³C isotopes respectively. As constituted, the MS of triazoles **2** and **4** and the corresponding triazolium salts **6** and **8** showed the presence of the bromide substituent. Bromine has two isotopes, ⁷⁹Br and ⁸¹Br in approximately 1:1 abundance ratio, compounds containing one bromine atom will show two peaks in the molecular ion region, depending on which bromine isotope the molecular ion contains [22]. The ⁷⁹Br isotope showed a base peak at [M]⁺ whereas those of ⁸¹Br were observed at [M+2]⁺. Important IR bands observed for the triazoles corresponded to the C–H stretch (3000–2850 cm⁻¹), =C–H stretch (3100–3000 cm⁻¹), C=C stretch (1680–1640 cm⁻¹) and C=O stretch (1750–1735 cm⁻¹). An absorption band at 1254–1131 cm⁻¹ was assigned to N=N of the neutral 1,2,3-triazoles [23]. The obtained EA results of the triazoles and corresponding salts correlated well to theoretical values within acceptable limits of deviation.

3.1. Single crystal structural analysis

Structural data of representative compounds **1**, **3**, **6**, and **8**, were

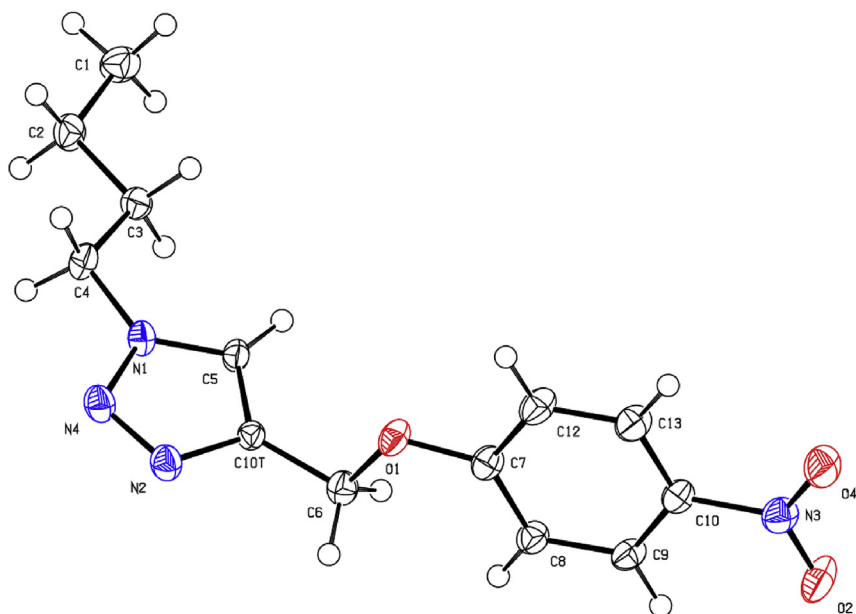


Fig. 4. ORTEP representation of the structure of **1** with the displacement ellipsoids drawn at the 50% probability level. Selected bond lengths (Å) and angles (°) N1–N4, 1.338(6); N1–C4 1.475(7); N1–C5 1.342(6); N4–N2 1.312(7); N4–N1–C5 110.7(4); N2–N4–N1 107.9(4); N2–C10T–C5 108.2(40).

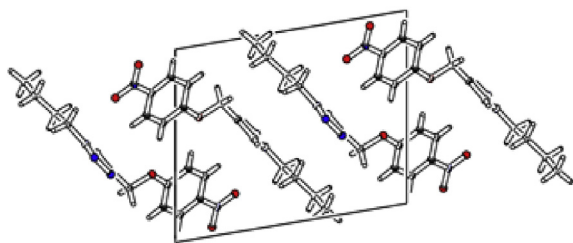


Fig. 5. Packing arrangement in a crystal of **1**.

determined from crystals grown in acetone/hexane solvent mixtures with atom numbering schemes depicted in Figs. 3–6

respectively. The crystal structures of the neutral triazole compounds **1** (Figs. 4) and **3** (Fig. 6) illustrated structural compositions consistent with the characterisation data discussed above with both compounds crystallizing in the P-1 space group of the triclinic crystal system [24]. All bond angles and lengths are within limits reported for related azolium compounds [25].

If the phenoxyethyl and straight chain (butyl group in **1** and ethyl acetate in **3**) wingtip substituents are respectively assumed as the ‘head’ and ‘tail’ of each molecule, then the packing arrangement of molecules in crystals of the neutral triazole compounds **1** and **3** may be described in terms of the interactions between these two moieties around each triazole unit. Interestingly, the packing arrangement in arrays of compound **1** (Fig. 5) is composed of

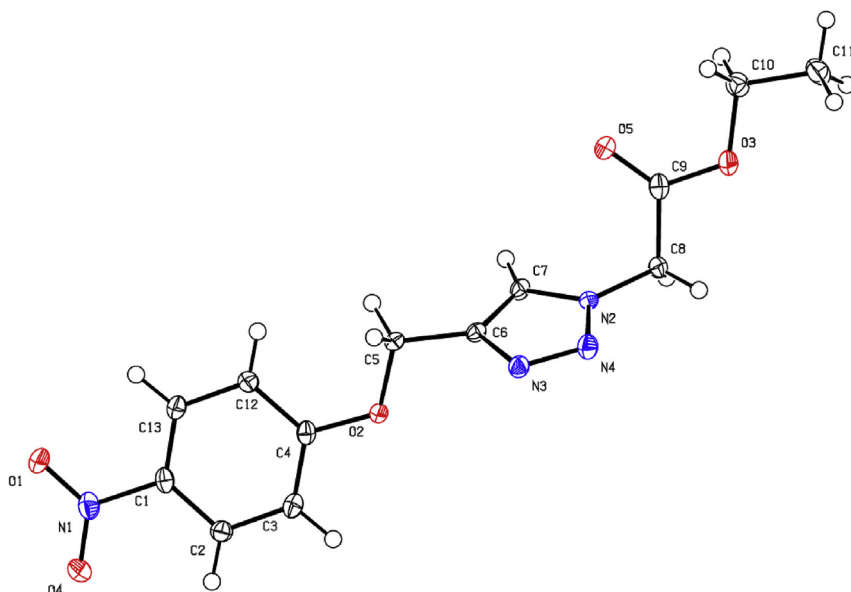


Fig. 6. ORTEP representation of the structure of **3** with the displacement ellipsoids drawn at the 50% probability level. Selected bond lengths (Å) and angles (°) N2–N4 1.342(3); N2–C7 1.3556(19); N2–C8 1.458(2); N4–N3 1.316(16); N3–C6 1.365(3); C6–C5 1.4931(16); C6–C7 1.368(3); N4–N2–C7 111.38(15); N3–N4–N2 107.3 (2); N2–C7–C6 103.9(2).

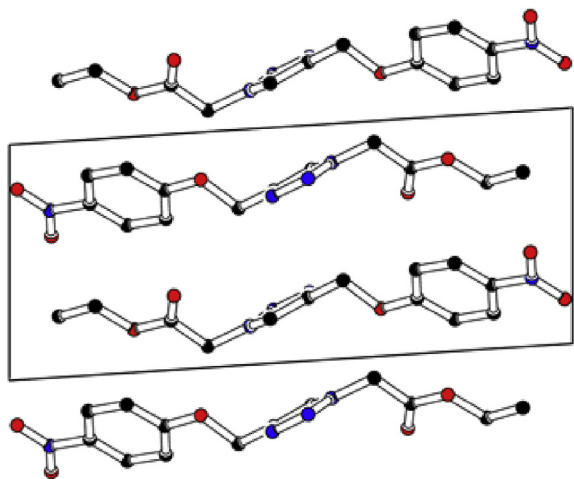


Fig. 7. Packing arrangement in a crystal of **3**.

repeating blocks of tail-to-tail then head-to-head units. This is a very efficient packing pattern that allows for minimal intermolecular and steric repulsion between neighboring moieties. However, an arrangement composed of only regularly alternating head-to-tail layers is observed in the packing of **3** shown in Fig. 7 with adjacent layers related through 180° rotation. This type of packing pattern is common in molecules with bulky side groups and helps to reduce inter-molecular repulsion and steric strain. In addition, this pattern is differentiated from that of compound **1** by the absence of intermolecular π - π interactions involving the N-phenoxyethyl moiety.

The triazolium salts **6** (Fig. 8) and **8** (Fig. 10) respectively belong to the monoclinic (space group $C2/c$) and triclinic (space group $P-1$) crystal systems. Interestingly, the structures of **6** and **8** showed non-classical long-range inter-halogen contacts at an angle of 180° separated by 3.735 and 3.692 Å respectively. This is a weak non-

covalent interaction that occurs when net attractive forces between a positively polarized halogen atom, frequently bromine or iodine exists in close proximity to a Lewis base [26].

Crystal packing in molecules of **6** and **8** are shown in Figs. 9 and 11 respectively. In compound **6**, a repeating zig-zag pattern is observed with the phenoxyethyl substituents pointing away from each other in order to minimize steric repulsions due to the many conformations of the phenyl rings as a result of free rotation along the C3–O2–C2 ethereal bond. The ethyl acetate tail ends of **8** packed in a similar fashion to the butyl N-substituent in **1** hence affording related packing patterns. It is also noteworthy that the quaternisation of the neutral triazoles to N-alkylated triazolium salts bearing delocalized positive charges has very little effect on the N–N bond lengths which are only slightly shorter in **6** and **8** when compared to **1** and **3**.

3.2. Catalytic transfer hydrogenation

In view of growing global concerns for the health of the environment and the need for the development of sustainable processes, we envisioned that triazolium based organocatalysts will share similarities in catalytic performance to related imidazolium analogues reported to be active in catalytic transfer hydrogenation (CTH) reactions [8]. Also, the stability and resistance of triazolium C(4,5) protons to deprotonation by bases is well-documented

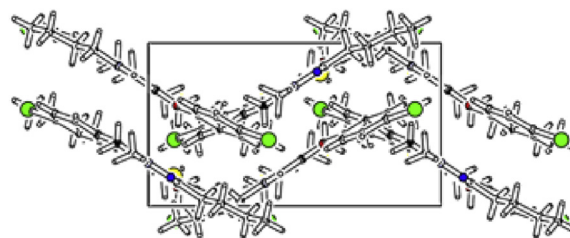


Fig. 9. Packing arrangement in a crystal of **6**.

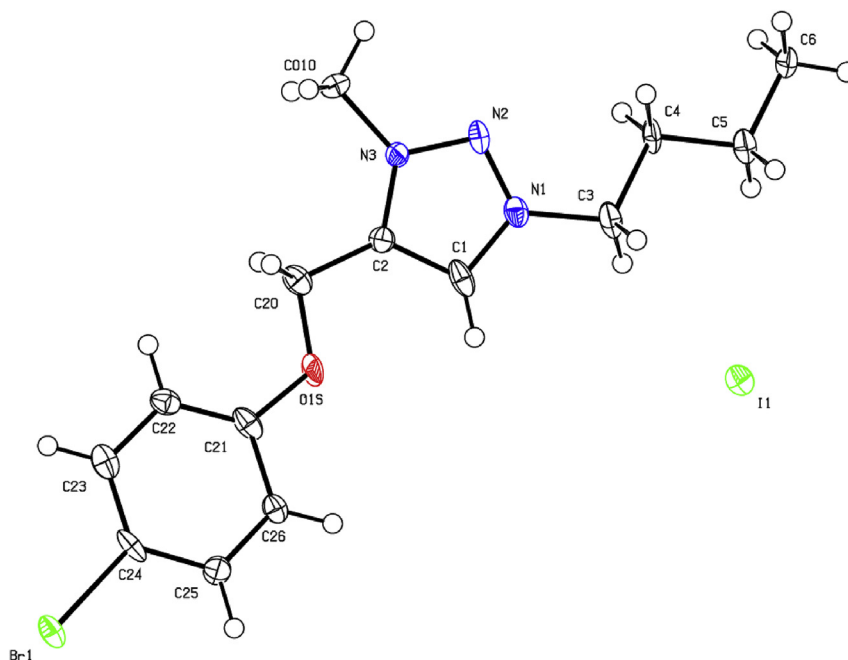


Fig. 8. ORTEP representations of the structure of **6** with the displacement ellipsoids drawn at the 50% probability level. Selected bond lengths (Å) and angles ($^\circ$) N1–N2 1.312 (13); N2–N3 1.323 (10); N3–C2 1.354 (11); C2–C1 1.396 (13); C1–N1 1.353 (11); N1–C3 1.498 (11); N1–N2–N3 104.4 (8); N2–N3–C2 112.7 (8); C3–N1–N2 113.6 (8).

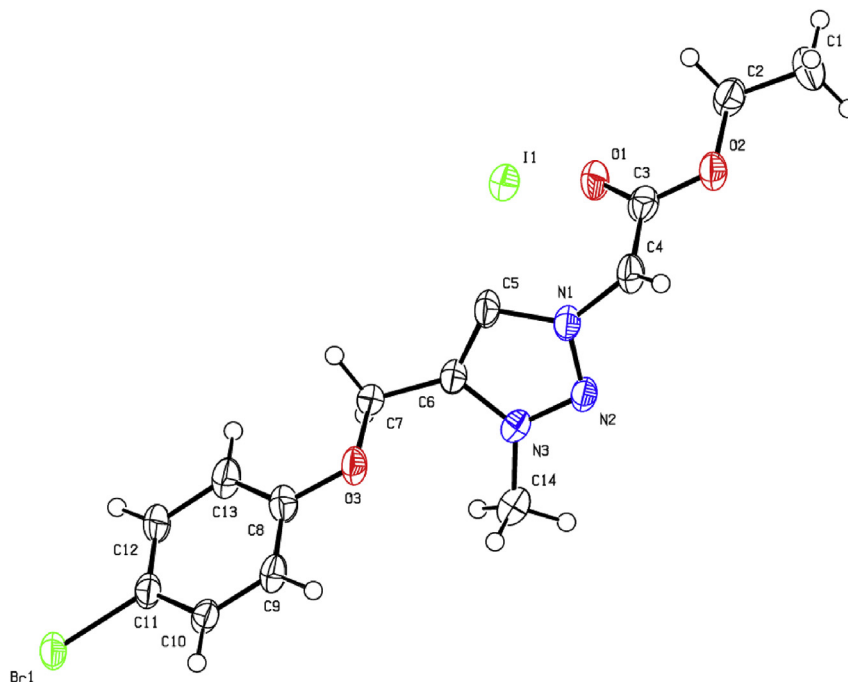


Fig. 10. ORTEP representations of the structure of **8** with the displacement ellipsoids drawn at the 50% probability level. Selected bond lengths (Å) and angles (°) N1–N2 1.326 (11); N2–N3 1.314 (11); N3–C6 1.370 (11); C6–C7 1.490 (12); C6–C5 1.376 (14); C5–N1 1.382 (11); N1–N2–N3 105.1 (7); N2–N3–C6 113.2 (8); C5–N1–N2 111.4 (8).

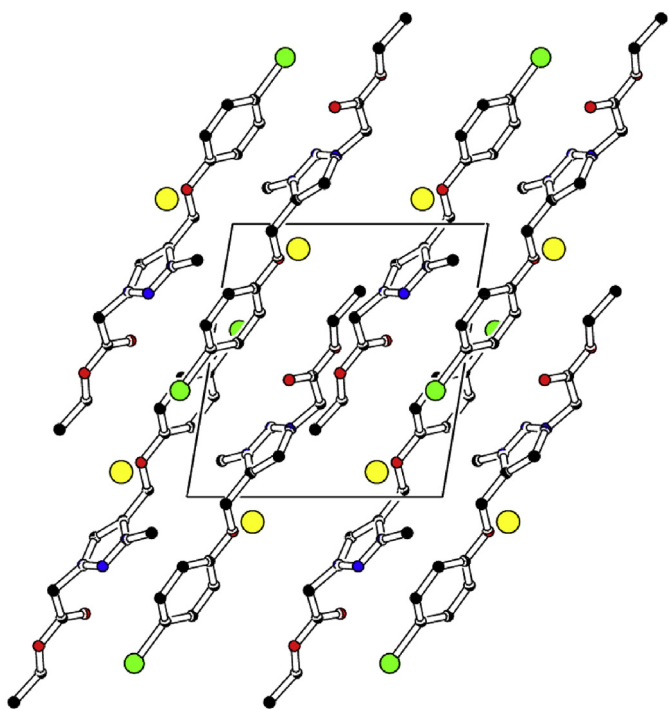


Fig. 11. Packing arrangement in a crystal of **8**.

which is in stark contrast to the susceptibility of the acidic imidazolium C(2) proton to attack under such conditions [4]. As a follow-up to our previous report on the use of imidazolium salts as organocatalysts for CTH, we hypothesized that triazolium salts will thus possess added advantages for CTH reactions that are promoted by inorganic bases such as KOH [8]. Hence, based on well-established procedures and techniques, we ran all the salts (**5–8**) on acetophenone as the model substrate at varying temperatures. From the

Table 1
Transfer hydrogenation of acetophenone catalyzed by triazolium salts **5–8**.

Entry	Organocatalyst	Conversion (%) ^a
1	5	56
2	6	41
3	7	65
4	8	58

Reactions were conducted in air at 82 °C using acetophenone (2.2 mmol), KOH (0.112 g) dissolved in 10 ml isopropanol.

^a Conversion was determined by GC analysis after 12 h. No reaction was recorded in the absence of KOH.

results presented in Table 1, entries 1–4 showed that all the salts were moderately active in the CTH protocol resulting in the conversion of acetophenone to phenylethanol with organocatalyst **7** showing the best conversion rate of 65%. In summary, triazolium salts bearing electron withdrawing *N,N*-substituents produced higher conversions to 1-phenylethanol, which we attributed to improved ability of the quarternised azolium salt to interact with the nucleophilic ketone substrate hence promoting reduction of the C=O bond.

After scanning a range of ketones, catalyst **7** was shown to be active for aromatic ketones bearing activating (electron withdrawing) groups *para* to the carbonyl, but poor for aliphatic ketones and aromatic ketones bearing sterically encumbering groups *ortho* to the C=O group.

4. Conclusion

In summary, a new series of azolium ionic compounds were prepared and the molecular structures of representative neutral 1,2,3-triazoles and corresponding salts were determined by a variety of techniques including single crystal XRD. The reported compounds may be used as sources of mesoionic carbene ligands for the synthesis of organometallic complexes or may be used as metal free organocatalysts for the activation of small molecules.

Acknowledgements

This project was funded by the National Research Foundation of South Africa and the University of KwaZulu-Natal for which we are grateful.

Appendix A. Supplementary data

Supplementary data to this article can be found online at <https://doi.org/10.1016/j.molstruc.2018.10.095>.

References

- [1] M.G.F. Hartmuth, C. Kolb, K. Barry Sharpless, Click chemistry: diverse chemical function from a few good reactions, *Angew. Chem. Int. Ed.* 40 (2001) 2004–2021.
- [2] J.K. Shah, H. Blumenthal, J. Liebscher, 1,2,3-triazolium-tagged prolines and their application in asymmetric Aldol and Micheal reactions, *Synthesis* 23 (2009) 3975.
- [3] P.N. Mathew, M. Albrecht, 1,2,3-Triazolylidenes as versatile abnormal carbene ligands for late transition metals, *J. Am. Chem. Soc.* 130 (2008) 13534–13535.
- [4] Y. Jeong, J.-S. Ryu, Synthesis of 1, 3-dialkyl-1, 2, 3-triazolium ionic liquids and their applications to the Baylis–Hillman reaction, *J. Org. Chem.* 75 (2010) 4183–4191.
- [5] H. Ibrahim, M.D. Bala, Improved methods for the synthesis and isolation of imidazolium based ionic salts, *Tetrahedron Lett.* 55 (2014) 6351–6353.
- [6] S. Diéz-González, S.P. Nolan, Stereoelectronic parameters associated with N-heterocyclic carbene (NHC) ligands: a quest for understanding, *Coord. Chem. Rev.* 251 (2007) 874–883.
- [7] S.G. Mncube, M.D. Bala, Recoverable aqueous-ionic liquid biphasic catalyst system for the oxidation of n-octane, *J. Mol. Liq.* 215 (2016) 396–401.
- [8] M.I. Ikhile, V.O. Nyamori, M.D. Bala, Transition metal free transfer hydrogenation of ketones promoted by 1, 3-diarylimidazolium salts and KOH, *Tetrahedron Lett.* 53 (2012) 4925–4928.
- [9] G.M. Sheldrick, A short history of SHELX, *Acta Crystallogr. Section A Found. Crystallogr.* 64 (2008) 112–122.
- [10] A.L. Spek, Single-crystal structure validation with the program PLATON, *J. Appl. Crystallogr.* 36 (2003) 7–13.
- [11] L.J. Farrugia, WinGX and ORTEP for windows: an update, *J. Appl. Crystallogr.* 45 (2012) 849–854.
- [12] Q. Zhang, H. Su, J. Luo, Y. Wei, “Click” magnetic nanoparticle-supported palladium catalyst: a phosphine-free, highly efficient and magnetically recoverable catalyst for Suzuki–Miyaura coupling reactions, *Catal. Sci. Technol.* 3 (2013) 235–243.
- [13] S. Bräse, C. Gil, K. Knepper, V. Zimmermann, Organic azides: an exploding diversity of a unique class of compounds, *Angew. Chem. Int. Ed.* 44 (2005) 5188–5240.
- [14] J. Albadi, M. Keshavarz, F. Shirini, M. Vafaie-nezhad, Copper iodide nanoparticles on poly(4-vinyl pyridine): a new and efficient catalyst for multi-component click synthesis of 1,4-disubstituted-1,2,3-triazoles in water, *Catal. Commun.* 27 (2012) 17–20.
- [15] N. Mukherjee, S. Ahammed, S. Bhadra, B.C. Ranu, Solvent-free one-pot synthesis of 1, 2, 3-triazole derivatives by the ‘Click’ reaction of alkyl halides or aryl boronic acids, sodium azide and terminal alkynes over a Cu/Al₂O₃ surface under ball-milling, *Green Chem.* 15 (2013) 389–397.
- [16] X. Creary, A. Anderson, C. Brophy, F. Crowell, Z. Funk, Method for assigning structure of 1,2,3-triazoles, *J. Org. Chem.* 77 (2012) 8756–8761.
- [17] G. Drake, G. Kaplan, L. Hall, T. Hawkins, J. Larue, A new family of energetic ionic liquids 1-amino-3-alkyl-1, 2, 3-triazolium nitrates, *J. Chem. Crystallogr.* 37 (2007) 15–23.
- [18] B.P. Mudraboyina, M.M. Obadia, I. Abdelhedi-Miladi, I. Allaoua, E. Drockenmuller, Versatile click functionalization of poly(1,2,3-triazolium ionic liquid)s, *Eur. Polym. J.* 62 (2015) 331–337.
- [19] D. Schweinfurth, S. Strobel, B. Sarkar, Expanding the scope of ‘Click’ derived 1,2,3-triazole ligands: new palladium and platinum complexes, *Inorg. Chim. Acta.* 374 (2011) 253–260.
- [20] D. Urankar, B. Pinter, A. Pevec, F. De Proft, I. Turel, J. Kosmrlj, Click-triazole N₂ coordination to transition-metal ions is assisted by a pendant pyridine substituent, *Inorg. Chem.* 49 (2010) 4820–4829.
- [21] J. Zhang, K. Higashi, K. Ueda, K. Kadota, Y. Tozuka, W. Limwikrant, K. Yamamoto, K. Moribe, Drug solubilization mechanism of α -glucosyl stevia by NMR spectroscopy, *Int. J. Pharm.* 465 (2014) 255–261.
- [22] D.K. Holdsworth, Mass spectra of organic compounds containing bromine and chlorine, *J. Chem. Educ.* 59 (1982) 780.
- [23] B. Garudachari, A.M. Isloor, M.N. Satyanarayana, H.-K. Fun, G. Hegde, Click chemistry approach: regioselective one-pot synthesis of some new 8-trifluoromethylquinoline based 1,2,3-triazoles as potent antimicrobial agents, *Eur. J. Med. Chem.* 74 (2014) 324–332.
- [24] I. Matulková, I. Némec, K. Teubner, P. Némec, Z. Mička, Novel compounds of 4-amino-1,2,4-triazole with dicarboxylic acids – crystal structures, vibrational spectra and non-linear optical properties, *J. Mol. Struct.* 873 (2008) 46–60.
- [25] D. Schweinfurth, R. Pattacini, S. Strobel, B. Sarkar, New 1,2,3-triazole ligands through click reactions and their palladium and platinum complexes, *Dalton Trans.* 42 (2009) 9291–9297.
- [26] J.M. Mercurio, R.C. Knighton, J. Cookson, P.D. Beer, Halotriazolium axle functionalised [2]Rotaxanes for anion recognition: investigating the effects of halogen-bond donor and preorganisation, *Chem. Eur. J.* 20 (2014) 11740–11749.